Available online at www.sciencedirect.com
SCIENCE DIRECT®
PERGAMON
Chaos, Solitons and Fractals 19 (2004) 55–60
CHAOS SOLITONS & FRACTALS
www.elsevier.com/locate/chaos

Rescaled range analysis and detrended fluctuation analysis study of cast irons ultrasonic backscattered signals

J. Mauricio O. Matos [a], Elineudo P. de Moura [b,*], Silvio E. Krüger [b], J. Marcos A. Rebello [b]

[a] *Department of Physics, Federal University of Ceará, P.O. Box 6030, CEP 60451970, Fortaleza, Brazil*
[b] *Department of Metallurgical and Materials Engineering, Federal University of Rio de Janeiro, COPPE/UFRJ, P.O. Box 68505, CEP 21495-970, Rio de Janeiro, Brazil*

Accepted 26 February 2003

Abstract

RS Analysis and DF Analysis have been applied to backscattered ultrasonic signals obtained from three different cast iron samples in order to investigate the fractal nature of the microstructure of these materials. The results show a scenario with two distinct regions whose calculated parameters can be used to estimate their fractal dimensions.

1. Introduction

Ultrasonic velocity and attenuation in plane parallel specimens are obtained by using a pulse-echo technique that measures the amplitude variation as a function of the transit time in backwall echoes. The obtained information has been widely used for materials characterization [1] but it is limited and specific. However, as an incident acoustic signal propagates within the material it is scattered by the microstructure and the resultant signal is very noisy. These backscattered signals certainly contain useful information of the microstructure and its spatial distribution. They show a highly irregular structure and in order to study them, attempting to characterize materials, one needs nonconventional statistical methods. Traditional approaches such as powerspectrum analysis present some difficulties when one wants to precisely quantify long-range correlations in nonstationary signals [2].

In this work we have applied the classical rescaled range analysis (RS) [3–5] and the detrended fluctuation analysis (DF) [6–9] to study ultrasonic backscattered signals from three different samples of cast iron: spheroidal (S), lamellar (L) and vermicular (V) graphite. (RS) and (DF) are scaling analysis methods that yield simple quantitative exponents H and α that are linked to the correlation properties of the signal and have been applied in a variety of research fields such as geophysics [5], cardiac dynamics, bioinformatics, economics, meteorology, material science, ethology, etc. [10–13]. Specifically, (RS) has been applied to characterize polycrystalline materials [14].

The outline of this paper is as follows. In Section 2 we review the algorithm of the (RS) and (DF) methods, in Section 3 we summarize the experiment, in Section 4 we present discuss the results and in Section 5 we present the conclusions.

* Corresponding author.
E-mail address: elineudo@metalmat.ufrj.br (E.P. de Moura).

0960-0779/04/$ - see front matter
doi:10.1016/S0960-0779(03)00080-8

2. RS and DF methods

Studying the Nile river and the problems related to water storage, Hurst created the (RS) method [15] which gives a reliable measure of some statistical aspects of time series records, as discussed by Mandelbrot [4] and Mandelbrot and Wallis [5]. Based on Feder [16], (RS) analysis can be introduced as follow.

Given a time series $\{x(1), x(2), \ldots, x(t)\}$ of a natural phenomena recorded at discrete time over a time span τ, we calculate the average influx over the period τ

$$\langle x \rangle_\tau = \frac{1}{\tau} \sum_{t=1}^{\tau} x(t). \tag{1}$$

Compute $X(t)$ as the accumulated departure of the influx $x(t)$ from the mean $\langle x \rangle_\tau$,

$$X(t,\tau) = \sum_{u=1}^{t} \{x(u) - \langle x \rangle_\tau\}. \tag{2}$$

The range R is defined as the difference between the maximum and minimum accumulated influx X,

$$R(\tau) = \max X(t,\tau) - \min X(t,\tau), \tag{3}$$

where $1 \leqslant t \leqslant \tau$. By using the standard deviation

$$S = \sqrt{\frac{1}{\tau} \sum_{t=1}^{\tau} \{x(t) - \langle x \rangle_\tau\}^2}, \tag{4}$$

Hurst found that the observed rescaled range, R/S, is very well described for a large number of natural phenomena by the following empirical relation:

$$\frac{R}{S} = (c\tau)^H, \tag{5}$$

where H is the Hurst exponent. For records generated by statistically independent processes with finite variance it can be shown that [17,18]

$$\frac{R}{S} = \left(\frac{\pi}{2}\tau\right)^{1/2}. \tag{6}$$

We can write Eq. (5) as follow:

$$\log_{10}(R/S) = H \log_{10}(\tau) + H \log_{10} c, \tag{7}$$

and by plotting $\log_{10}(R/S)$ against $\log_{10}(\tau)$ one can obtain, in the scaling region, a straight line whose slope is the Hurst exponent H. The relation between the Hurst exponent and the box counting fractal dimension is simply [18]

$$D = 2 - H. \tag{8}$$

From Eqs. (6) and (8) we can see that for statistically independent fractional Brownian movement, with $H = 0.5$, the fractal dimension should be $D = 1.5$. A Hurst exponent of $0.5 < H < 1.0$ corresponds to a profile like curve showing persistent behavior, while for $0 < H < 0.5$, we have an antipersistent behavior.

(DF) analysis is well described in references [6–8] and has been recently reviewed [19]. Briefly, it can be introduced as follow. Given a time series $\{x(1), x(2), \ldots, x(t)\}$, let us integrate the time series $\{x(i)\}$

$$y(j) = \sum_{i=1}^{j} [x(i) - \langle x \rangle], \tag{9}$$

Now we divide the entire sequence into equal intervals, and define a local trend for each interval to be the ordinate of a linear-squares fit for the $y(j)$'s, in that interval. Next we define the detrended value, denoted by $y_l(j)$, as the difference between the original $y(n)$'s and the local trend in an interval of length l. The variance about the detrended value for each interval is calculated, as well as the average of these variances over all intervals of size l, denoted by $F_d(l)$. By plotting $\log_{10}(F_d(l))$ against $\log_{10}(l)$, we get a straight line whose angular coefficient is the α exponent [19]. In many cases α is very close to H [7] and also satisfies Eq. (8).

3. The experiment

In order to obtain the backscattered signals for (RS) and (DF) analysis of the lamellar (L), vermicular (V) and spheroidal (S) graphite, a broad band ultrasonic probe with central frequency of 5 MHz was used to emit a short pulse of ultrasound towards the sample and record the signal reflected back from various acoustic boundaries within the

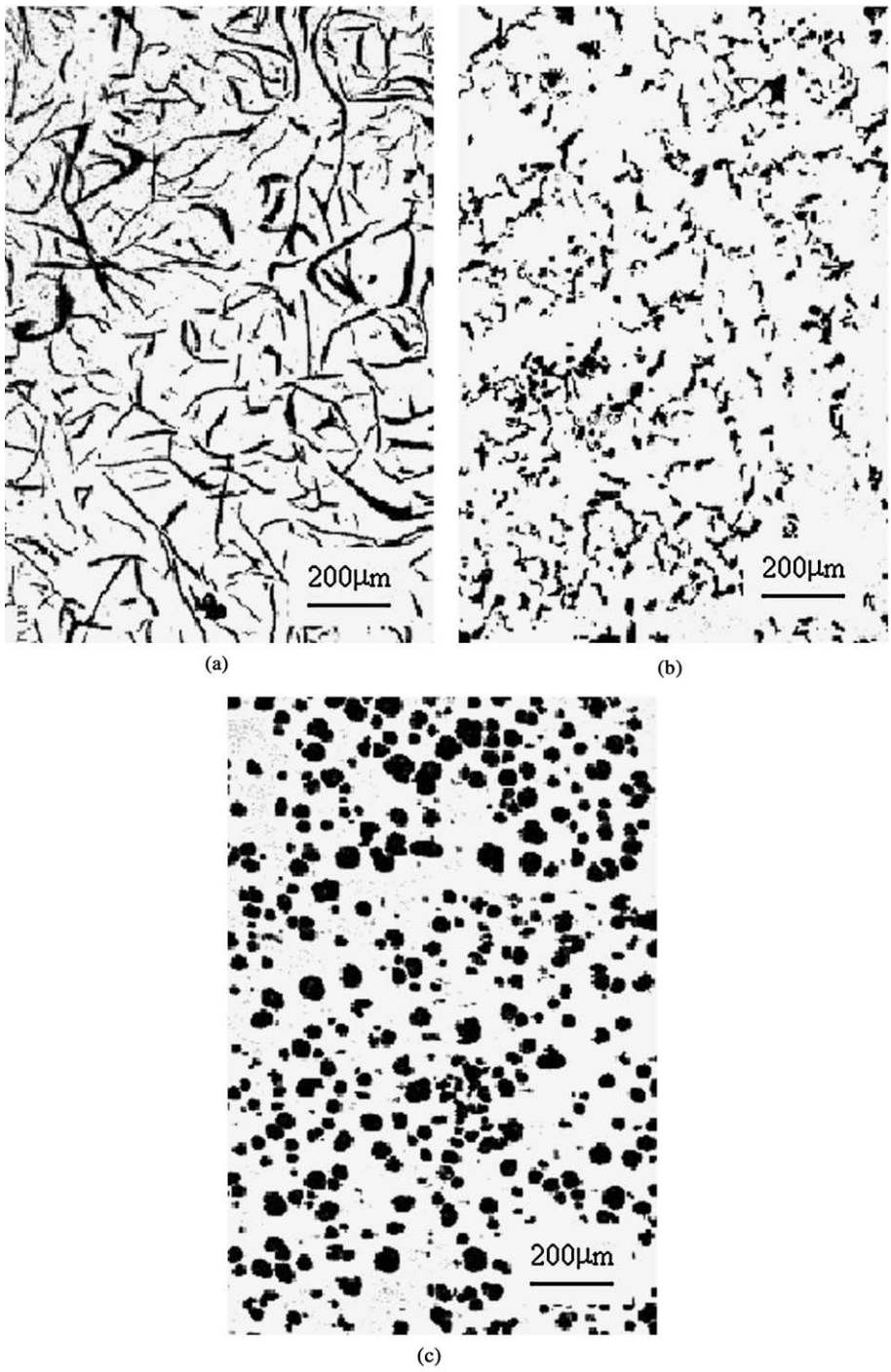

Fig. 1. (a) Micrograph of lamellar cast iron (L). (b) Micrograph of vermicular cast iron (V). (c) Micrograph of spheroidal cast iron (S).

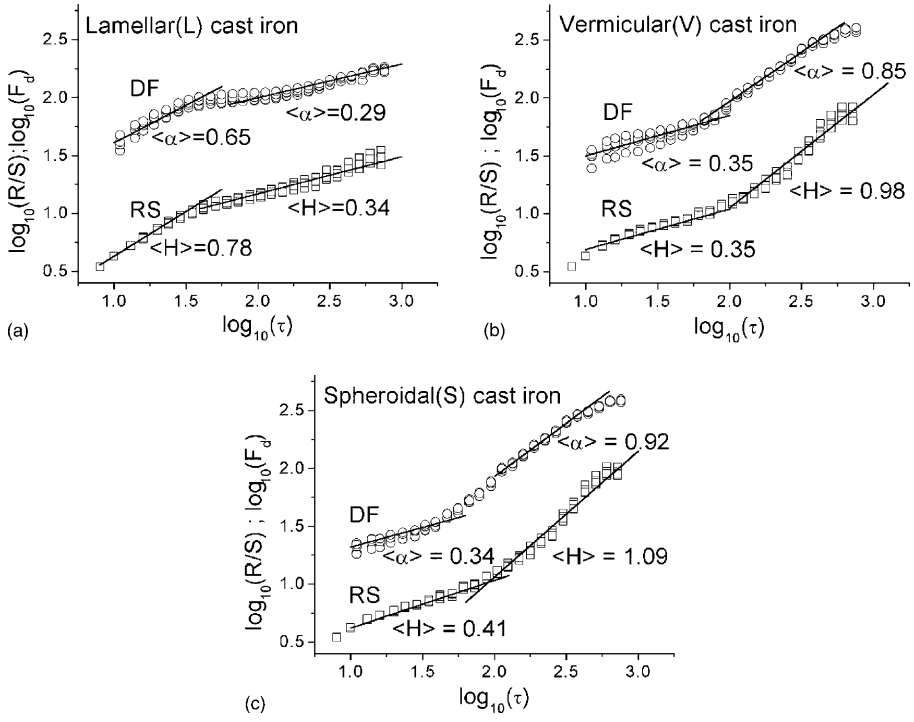

Fig. 2. (a) (RS) and (DF) results for lamellar cast iron. (b) (RS) and (DF) results for vermicular cast iron. (c) (RS) and (DF) results for spheroidal cast iron.

samples. While the signals were recorded, the position of the probe on each sample was changed randomly 40 times and a backscattered signal of 512 points, at each position, was registered at a sampling rate of 40 M samples/s. From these 40 backscattered signals, eight individual signals were then combined, following a procedure adopted in reference [20], to form five groups of signals with 4096 data points for each sample.

4. Results and discussion

Fig. 1 shows micrographs of the three samples, lamellar (L), vermicular (V), and spheroidal (S) graphite, that have been submitted to pulse-echo techniques and whose backscattered signals were studied by (RS) and (DF) analysis.

Fig. 2 shows the results of this (RS) and (DF) analysis. The points on the plot were computed by (RS) and (DF) analysis of five representative sets of each sample. Each set comprises 4096 data points, collected from the corresponding sample. For each (RS) and (DF) set of points a least square linear fit was performed and yielded five (RS) and (DF) exponents. The mean value of $\langle H \rangle$ and $\langle \alpha \rangle$ for each case is displayed in Fig. 2.

Fig. 2 clearly shows two regions in all three cases of the cast iron studied. This implies that there are two different time scales and characterizes these materials as multifractals. In the first region, small τ, we are measuring the fine scale structure of the signal, while in the second region we are measuring the larger scale of the signal. The (RS) and (DF) results are consistent and show the same trend in all cases. Associated to these regions we have a fine structure dimension (D_{fs}), that estimates the fractal character of the graphite, and a large structural dimension (D_{ls}), associated with the distribution of the microstructure. In Table 1 we display these dimensions computed by using Eq. (8) and taking the mean value of H and α for each region.

It is interesting to note that mechanically lamellar or gray iron is weak and brittle compared to vermicular or malleable iron and spheroidal or ductile iron. The microstructures of the last two cast irons are similar which accounts for their relative strength and appreciable ductility or malleability. The entries of Table 1 are consistent with these mechanical characteristics: the fractal dimensions of vermicular and spheroidal irons are very close and $D_{\mathrm{fs}} > D_{\mathrm{ls}}$ while the lamellar dimensions differ substantially from the other two and $D_{\mathrm{ls}} > D_{\mathrm{fs}}$.

Table 1
(D_{fs}) and (D_{ls}) dimensions of cast irons

Cast iron	D_{fs}	D_{ls}
L	1.29	1.69
V	1.65	1.09
S	1.63	1.01

5. Conclusion

We have attempted to investigate the fractal nature of the ultrasonic backscattered signals from three different cast iron samples. In all cases the yielded results show a scenario with two distinct regions where the calculated (RS) and (DF) parameters are used to estimate their fractal dimensions. The vermicular and spheroidal backscattered signals are antipersistent in the fine scale region and persistent in the large scale region. In contrast, the lamellar signals are persistent in the fine scale region and antipersistent in the large scale region. The cast iron samples studied are thus examples of systems with multifractal properties. Finally, it is worthwhile pointing out that lamellar cast iron has different mechanical properties as compared to other cast iron samples [21] and that (RS) and (DF) analyses are promising methods for material characterization.

Acknowledgements

We gratefully acknowledge fruitful discussions with Prof. Lindberg L. Gonçalves and the financial support of the Brazilian agencies CAPES and FINEP.

References

[1] Sullivan PF, Papadakis PE. Ultrasonic Double Refraction in Worked Metals 1961;33(11):1622–4.
[2] Kantz H, Schreiber T. Nonlinear Time Series Analysis, Cambridge Nonlinear Science Series, No. 7, Cambridge University Press, 1997.
[3] Hurst HE, Black RP, Simaika YM. Long-Term Storage: An Experimental Study. London: Constable; 1965.
[4] Mandelbrot BB. The Fractal Geometry of Nature. New York: W.H. Freeman & Company; 1983.
[5] Mandelbrot BB, Wallis JR. Some long-run properties of geophysical records. Water Resources Research 1969;5(2):321–40.
[6] Peng CK, Buldyrev SV, Havlin S, Simon M, Stanley HE, Goldberger AL. Mosaic organization of DNA nucleotides. Physical Review E 1994;49(2):1685–9.
[7] Moreira JG, Kamphorst Leal da Silva J, Oliffson Kamphorst S. On the fractal dimension of self-affine profiles. Journal of Physics A 1994;27:8079–89.
[8] Buldyrev SV, Goldberger AL, Havlin S, Peng CK, Stanley HE, et al. Fractal landscapes and molecular evolution: modeling the myosin heavy chain gene family. Biophysical Journal 1993;65:2673–9.
[9] Taqqu MS, Teverovsky V, Willinger W. Estimators for long-range dependence: an empirical study. Fractals 1995;3(4):785–98.
[10] Iyengar N, Peng CK, Morin R, Goldberger AL, Lipsitz LA. Agerelated alterations in the fractal scaling of cardiac interbeat interval dynamics. American Journal of Physiology 1996;271:1078–84.
[11] Peng CK, Buldyrev SV, Goldberger AL, Havlin S, Simon M, Stanley HE. Finite-size effects on long-range correlations: implications for analyzing DNA sequences. Physical Review E 1993;47(5):3730–3.
[12] Ivanova K, Ausloos M. Application of the Detrended Fluctuation Analysis (DFA) method for describing cloud breaking. Physica A 1999;274:349–54.
[13] Kantelhardt JW, Berkovits R, Havlin S, Bunde A. Are the phases in the Anderson model long-range correlated. Physica A 1999;266:461.
[14] Barat P. Fractal characterization of ultrasonic signals from polycrystalline materials. Chaos, Solitons & Fractals 1998;9(11):1827–34.
[15] Hurst HE. Long-term storage capacity of reservoirs. Transactions of the American Society of Civil Engineers 1951;116:770–99.
[16] Feder J. Fractals. New York: Plenum Press; 1988.
[17] Feller W. The asymptotic distribution of the range of sums of independent random variables. Annals of Mathematical Statistics 1951;22:427.
[18] Addison PS. Fractals and Chaos. London: IOP; 1997.

[19] Kun Hu, Plamen Ch. Ivanov, Zhi Chen, Pedro Carpena H. Eugene Stanley, Effect of Trends on Detrended Fluctuation Analysis, Physical Review E 2001;64:011114-7.
[20] Barat P, Mukherjee P, Dutta D. Fractal characterization of back scattered ultrasonic signals, in: 14th Word Conference on Non Destructive Testing (14th WCNDT), New Delhi, India, 8–13 December 1996.
[21] Kruger SE. Microstructural characterisation of cast iron by ultrasound, PhD Thesis (in Portuguese), COPPE, Federal University of Rio de Janeiro, Brazil, 2000.